IEEE Access
Multidisciplinary | Rapid Review | Open Access Journal

Received January 13, 2019, accepted February 3, 2019, date of publication February 12, 2019, date of current version February 27, 2019.

Digital Object Identifier 10.1109/ACCESS.2019.2898424

A Real-Time Queue Length Estimation Method Based on Probe Vehicles in CV Environment

HAIQING LIU[1], (Member, IEEE), WENLI LIANG[1], LAXMISHA RAI[2], (Senior Member, IEEE), KUNMIN TENG[1], (Student Member, IEEE), AND SHENGLI WANG[3],[4]

[1]College of Transportation, Shandong University of Science and Technology , Qingdao 266590, China
[2]College of Electronics, Communication and Physics, Shandong University of Science and Technology, Qingdao 266590, China
[3]Ocean Science and Engineering College, Shandong University of Science and Technology, Qingdao 266590, China
[4]Shandong Astro-Compass Information Technology Co., Ltd., Jinan 250108, China

Corresponding author: Shengli Wang (shlwang@sdust.edu.cn)

This work was supported in part by the Scientific Research Foundation of the Shandong University of Science and Technology for Recruited Talents under Grant 2017RCJJ054, and in part by the High-Level Innovation Fresh Talents From Home and Abroad, Jinan, under Grant 2016002.

ABSTRACT The real-time traffic status estimation in urban signalized intersections is highly valuable for modern traffic control and management. This paper presents a real-time queue length estimation method based on probe vehicles' data in the connected vehicle (CV) environment. The probe data are used to identify the stopping states of CVs. Based on this, a queue length time series referring to the stopping time and the positions of CVs is built for describing the queuing process at an intersection. Considering the statistical average traffic rate, queue length time series in historical cycles, and the stopping states for real-time CV arrival features in the current cycle, the critical queuing time is forecasted based on the linear fitting method and the real-time queue length is estimated based on the Markov model. The overall scheme is thoroughly tested and demonstrated in a realistic scenario at different penetration rates. Under different conditions, the stationarity of the queue length series is tested by the augmented Dickey–Fuller. Two Markov models based on the transition matrices of the current cycle and both the current and historical cycles are verified, respectively. The results demonstrate the high accuracy in the real-time queue length estimation, and the proposed method shows good performance in handling the randomness, especially when the CV penetration rate is low.

INDEX TERMS Connected vehicle, Markov model, queue length, time series.

I. INTRODUCTION

Real-time road traffic parameter collection and accurate road congestion evaluation are the prerequisites for better applying various Advanced Traffic Management System (ATMS) applications, such as traffic signal control, traffic guidance, traffic state forecasting and traffic accident identification. Traditional traffic parameter collection methods by transect-detectors [1]–[6] can only obtain the traffic information where the detector locates, mainly the vehicular throughput, speed and occupancy. Some procedural parameters which can describe the traffic status of an entire road segment or intersection and are more useful for deploying ATMS applications, such as the queue length, traffic delay and number of stops, are not easily obtained. In actual engineering applications, the drawbacks in comprehensiveness, accuracy and real-time of traffic parameter collection methods have become the 'bottleneck' for taking full advantage of the aforementioned advanced intelligent applications while improving the traffic flow.

Recently, with the development of wireless communication and intelli-sensing technologies, the connected vehicle (CV) system has been attracted much attention from scholars. For CV, the entire space-time driving state is obtained by all kinds of onboard sensors and the trajectory information can be transmitted to the data-centric processing system for further analysis. In the CV environment, the introduction of some probe data, such as the position, speed, accelerated speed of CVs, provides new data source for traffic status evaluation. This makes it possible to mine the real-time procedure traffic parameters which cannot be obtained in the traditional pattern. In recent years, for fully using the CV information,

The associate editor coordinating the review of this manuscript and approving it for publication was Arun Prakash.

many researches focusing on the traffic parameter evaluation, such as vehicle density [7]–[11], travel time [12]–[14] and origin-destination trip matrices [15], [16], have been presented for different applications.

Queue length is one of the most important performance measures of an intersection, as it reflects the delay and travel time at the intersection and is widely used in traffic signal plan design, traffic congestion evaluation, non-stopping speed guidance. The first study on queue length dates back to the use of probe vehicle, another form of CV. Comert and Certin [17], [18] use the location of the last probe vehicle in the queue length as well as the probability function to evaluate the expectation of queue length. A queue length estimation model is presented based on the penetration ratio. However, the probability function of total queue must be obtained for the proposed model. In [19], a cycle-by-cycle queue length estimation method by means of shock wave theory and probe vehicle data is proposed. This kind of probability-based method or shock wave theory based method generally gives a statistical queue length estimation value under the given probability assumptions. Due to the data quality of the probe vehicle, for example, the long term sampling interval and the low data accuracy, the estimation result is generally not satisfactory.

Using the trajectory information entirely, mainly the position and speed, some real-time queue length estimated methods are also presented. Tiaprasert *et al.* [20] present a mathematical model for real-time queue estimation using connected vehicle technology from wireless sensors networks. The calculation of estimated queue length begins with joint probability function of the total number of vehicles and connected vehicles. However, the proposed model is based on the assumption that the probability of the connected vehicle follows Bernoulli distribution, which is not able to perfectly describe the random characteristics of traffic flow, especially when the CV penetration is low. In order to achieve the overflow control, a maximum queue length calculation method is proposed in [21]. By tracking the variation of the speed of the CVs, the stop state is identified and the maximum queue length is denoted as farthest position of stopped CVs. In the proposed method, a full coverage of the CVs is needed if the system expects to get an accurate estimation result.

In actual applications, the penetration rate is really a challenge for designing a reliable model, especially in the early stage of implementation of CV engineering [22]–[24]. Fully considering the low penetration of CV in road traffic, a queue tail location estimation model is presented in [25]. In the model, the whole link is divided into upstream and downstream of queue tail. A rough estimation of queue tail based on connected vehicle located at farthest from downstream end of link, together with an error compensation scheme based on the penetration rate and number of lanes, are presented. It demonstrates the efficiency and accuracy of high-resolution estimation approach.

Summarizing the research on queue length estimation methods based on probe data mentioned above, we can also realize that, there are very few studies which present a comprehensive strategy for dealing with the random characteristics of traffic flow. In actual scenario, especially when the traffic is unsaturated, the traffic volume and arriving/releasing features all dynamically change at any time. The traffic characteristics may be quite different even in two different adjacent signal cycles. Sometimes there may be sharp increase or decrease in traffic volume compared with the statistical average value. In this case, some assumptions may be no longer appropriate and the effectiveness of corresponding queue length estimation models will surely be reduced [26].

For fully extracting the value of the probe data of CVs and to address the issues existing in the current traffic parameter evaluation methods, this paper proposes a new real-time queue length estimation method at signalized intersection under unsaturated traffic condition. The stopping states of CVs, including the complete stopping and incomplete stopping, are identified based on the probe data of CVs. Under certain penetration, the critical queuing time is forecasted. Further, a queue length time series model is built to describe the evolution of vehicle arriving and releasing characteristics. Using the Markov method, the series is analyzed and the real-time queue length is estimated. The overall scheme is thoroughly tested and demonstrated in a realistic scenario at different penetration rates. The results demonstrate the real-time behavior and accuracy for high-resolution estimation.

The rest of the paper is organized as follows. In Section 2, the survey of the method is briefly introduced. In Section 3, a real-time queue length forecasting method based on Markov Model is proposed, including the construction of queue length time series, forecasting of critical queuing time and optimization of state transition matrix for further queue length estimation. The case study and the evaluation results are presented in Section 4. In Section 5, we conclude the paper and provide the directions for future work.

II. METHOD DESCRIPTION

In the CV environment, each intelligent vehicle which is equipped with onboard sensors and wireless transmitting devices and can be considered as probe vehicle. The stopping state of the CV, which is critical for estimating the real-time queuing length of road section, can be identified using the real-time trajectory data. Generally, the vehicle stopping state can be classified into two types: complete stopping and incomplete stopping.

A. COMPLETE STOPPING

Blocked by the red light, vehicles wait in line and join the queue in turn. When a CV arrives and the front queue has not completely discharged, it should slow down the speed to zero and remain in the stopped state for a certain time d_k (d_k equals to the sum of the waiting time for the red light and the time of queue discharge, $d_k > 0$), as shown in Fig. 1. When a CV is complete stopping, it means that the standing queue spreads to the position where the CV locates and it may extend farther.

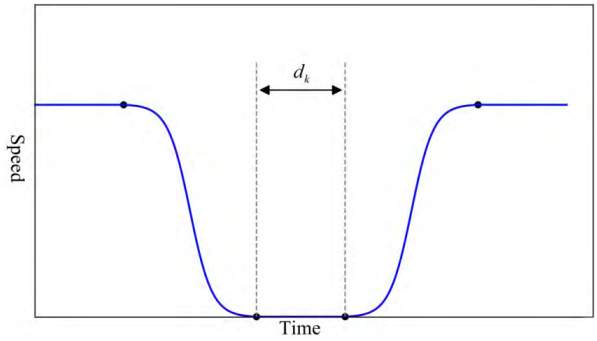

FIGURE 1. Complete stopping state identification based on speed variation.

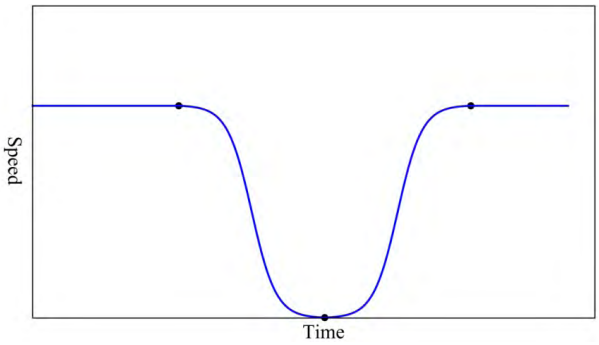

FIGURE 2. Incomplete stopping state identification based on speed variation.

B. INCOMPLETE STOPPING

When a CV slows down to the tail of the queue and the front vehicle is about to start, it has to speed up again to recover the normal running state in the next moment. In this situation, the parking time $d_k = 0$, as shown in Fig. 2. When a CV is in the state of incomplete stopping, it means that the standing queue spreads to the position where the CV located, and the following vehicles no longer need to stop.

When the CV is blocked by traffic signal light and queues in turn, the stopping position of the CV is exactly the instantaneous queuing place for traffic flow in the intersection entrance lanes. As shown in Fig. 3, the vehicles stopped behind the stopping line during the red time period. Among all vehicles, the CVs which are completed stopped make probe points for describing the queuing characteristics. By detecting the stopping time t_k and position L_k of CVs, a queue length variation series can be formed, that is $\{L_1(t_1), L_2(t_2), \cdots, L_k(t_k), \cdots, L_\dagger(t_\dagger)\}$, reflecting the real-time queuing progress dynamically. In the series, $L_\dagger(t_\dagger)$ is the critical queue length at the critical queuing time, denoting the farthest queue state in one signal cycle where the queue buildup wave meets the queue discharge wave. In this paper, the pivotal idea of the proposed method is using the time series analysis and forecasting approach for evaluating the real-time queue length in a traffic signal cycle.

III. A REAL-TIME QUEUE LENGTH FORECASTING METHOD BASED ON MARKOV MODEL

A. CONSTRUCTION OF THE QUEUE LENGTH TIME SERIES

The mathematical description for queue length variation of an intersection is the basis for forecasting the real-time traffic states. In this paper, we use the number of queuing vehicles to describe the queue length for further analysis. The queue length time series is built by (1):

$$Q = \{q(t_1), \cdots, q(t_m), \cdots, q(t_M)\} \tag{1}$$

where M denotes the number of elements in the series. $t_1, \cdots, t_m, \cdots, t_M$ are the equidistant time points. $q(t_m)$ is the number of queuing vehicles at t_m.

The t_m is expressed as follows:

$$t_m = m\Delta T = m(t_N/q_N) \tag{2}$$

where ΔT denotes the average stopping interval, which is a statistical value calculated by the stopping time t_N of the last detected CV (the N-th CV) and the queuing number q_N at the stopping time in certain historical signal cycles. Taking the ΔT as a time step, the whole signal cycle is segmented into $M = \lceil C/\Delta T \rceil$ time intervals.

Accordingly, the queuing state of the road section is segmented into $q_{\max}$ continuous intervals by unit 1, in which $q_{\max}$ denotes the maximum accommodating vehicles in the road section. In summary, the $q_{\max}$ continuous intervals represent the state space for the queuing length variations.

In one traffic signal cycle, the data-centric processing system receives the trajectories of N CVs and identifies the stopping states, including the stopping time, parking duration time, leaving time, queue length and the number of queuing vehicles, which are expressed as follows:

Stopping time series for N CVs:

$$T_B^s = \{t_1^s, \cdots, t_k^s, \cdots, t_N^s\} \tag{3}$$

Parking duration time series:

$$D_B = \{d_1, \cdots, d_k, \cdots, d_N\} \tag{4}$$

Leaving time series:

$$T_B^r = \{t_1^r, \cdots, t_k^r, \cdots, t_N^r\} \tag{5}$$

Queue length series (the distance between the vehicle and stop-line, of which the location information is acquired by positioning devices, such as GPS):

$$P_B = \{L_1, \cdots, L_k, \cdots, L_N\} \tag{6}$$

The number of queuing vehicles series:

$$Q_B = \{q_1, \cdots, q_k, \cdots, q_N\} \tag{7}$$

In (7),

$$q_k = \lceil L_k/H \rceil \tag{8}$$

In (8), H is the statistical average space headway when vehicles queue at the intersection. $\lceil * \rceil$ is the symbol for rounded integer calculation.

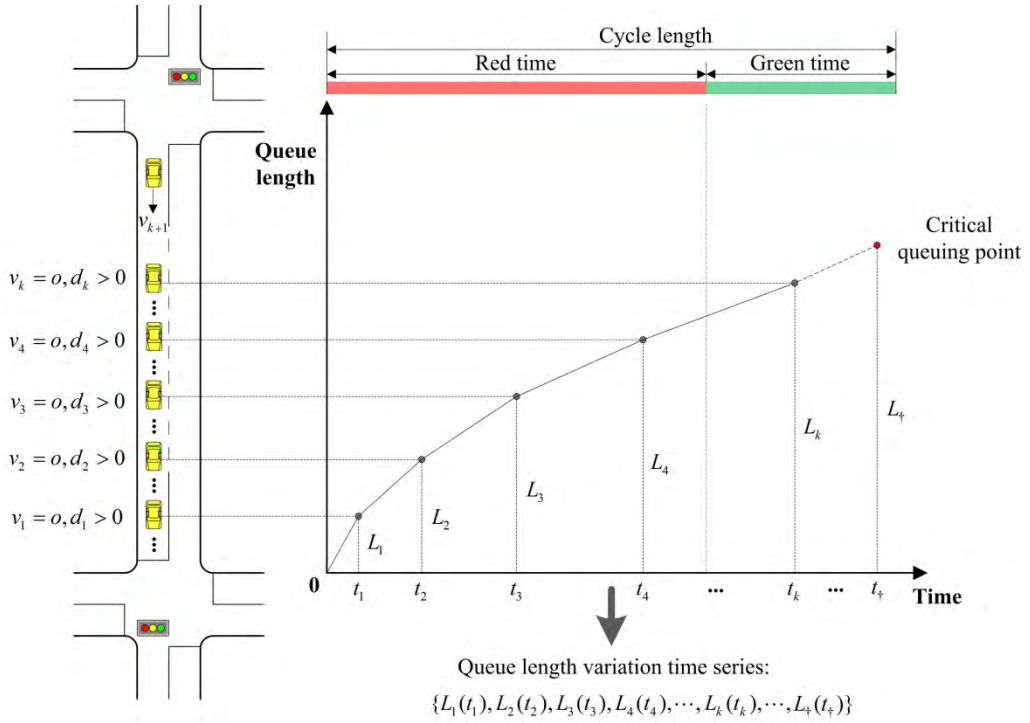

FIGURE 3. Queuing process based on CVs.

Based on the identification of stopping state of CV, the time series analysis method is used to describe the queuing states and forecast the real-time queue length. The arrival time and distributions in the queue present heterogeneous characteristics due to random characteristics of traffic flow. In Q, if one CV happens to arrive in the M-th time interval, the state of t_m equals to the number of queuing vehicles when the vehicle stops. For other time intervals, a data compensation method is proposed to make the time series complete as follows:

Suppose the k^{th} probe vehicle stops in the i^{th} time interval with the queuing state q_k, and the $(k+1)^{\text{th}}$ CV stops in the j^{th} time interval with the queuing state $q_{k+1}(j > i)$, the queuing states of the $(j-i-1)^{\text{th}}$ time intervals between i and j are lacking. For these intervals, the state calculation equation is built for data compensation, as shown in (9).

$$\begin{cases} q(t_i) = q_k \\ q(t_j) = q_{k+1} \\ q(t_{i+l}) = \lceil (q_{k+1} - q_k) l/(j-i) + q_k \rceil \\ \qquad\qquad l = 1, 2, \cdots, j-i-1 \end{cases} \tag{9}$$

The construction process of the queue length time series is described in Fig. 4

In Fig. 4, we can intuitively find that, according to the intersection queuing mechanism, the state presents progressive increase as the time grows in the queue length time series. This kind of time series consequentially shows non-stationary characteristics.

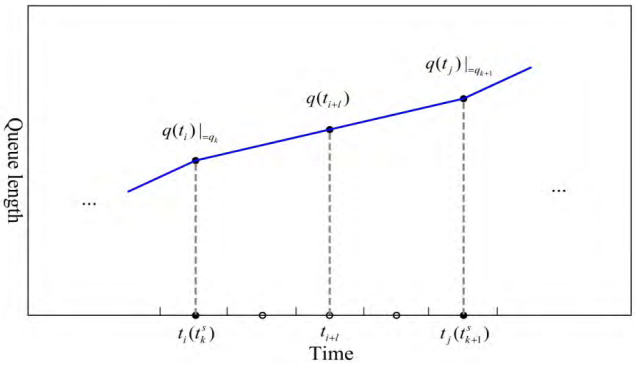

FIGURE 4. The construction of the queue length time series.

B. CRITICAL QUEUING TIME FORECASTING BASED ON CVs

The CVs send the trajectories to the data-centric processing system. The system identifies the vehicles which have an integrated parking process (IPP) based on the trajectories and stopping information, in which the IPP is defined as a whole parking process includes stopping, parking and restarting. Referring to the queue buildup and discharge characteristics in actual scenario, the parking time series presents a declining trend, as is shown in Fig. 5.

The stopping time series is fitted using a linear method and the fitting function is presented in (10).

$$d(t) = at + b \tag{10}$$

In (10), the parameters a and b are demarcated according to the minimum mean square error between fitted value and

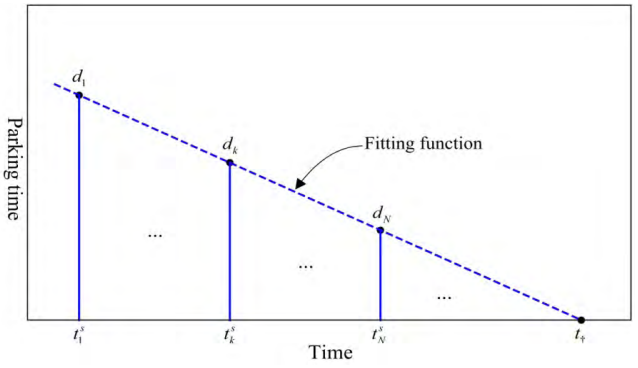

FIGURE 5. Parking time trend for integrated parking vehicles.

actual value principle, which is shown in (11).

$$\min Q(a,b) = \min \sum_{k=1}^{N-1} (d(t_k) - d_k)^2 = \min \sum_{k=1}^{N-1} (at_k + b - d_k)^2 \tag{11}$$

In (11), when $d(t_\dagger) = 0$, the critical queuing time $t_\dagger$ can be obtained.

While using the aforementioned method to forecast the critical queuing time, one necessary prerequisite is that the system must receive the IPP information from part of the CVs. Theoretically, as long as two samples are acquired, the fitting function is able to be established. Higher the samples are, the more accurate the function shows to forecast the critical queuing time. However in actual scenario, there may be very few, even no vehicle which can meet the IPP conditions when forecasting the critical queuing time. When such situation happens, the fitting model accumulates large error and even may become useless.

In order to solve the problem presented above, this paper proposes a reference point $t_\dagger^h$ for forecasting the critical queuing time of present cycle using the historical values of latest N_C signal cycles. The reference point considers two factors, the forecasting critical queuing time based on the historical N_C values and confidence level for the distribution of the historical values respectively.

In the historical signal cycles, all CVs' trajectories are obtained and they certainly meet the IPP conditions. The final critical queuing time series for the latest N_C cycles is expressed by (12):

$$T_\dagger = \{t^h_{\dagger(1)}, \cdots, t^h_{\dagger(k)}, \cdots, t^h_{\dagger(N_C)}\} \tag{12}$$

Besides, we assume that the distribution of the elements in $T_\dagger$ follows the normal distribution $N(\overline{t_\dagger}, \sigma^2)$.

Based on the historical critical queuing time values, the value for the current cycle is firstly forecasted using the linear fitting method, as follows:

$$t_\dagger^h = f_{lf}(t^h_{\dagger(1)}, \cdots, t^h_{\dagger(k)}, \cdots, t^h_{\dagger(N_C)}) \tag{13}$$

where f_{lf} is the fitting function, referring to (10) and (11).

In order to decrease the estimation error, the confidence level for the distribution of the historical values is used to modify the preliminary forecasting result. Let $\overline{\theta}$ and $\underline{\theta}$ represent the upper and lower boundary values of the confidence interval for historical N_C critical queuing time values under $1-\alpha$ confidence level, then,

$$(\overline{\theta}, \underline{\theta}) = (\overline{t_\dagger} - \frac{\sigma}{\sqrt{N_C}}\mu_{\alpha/2}, \overline{t_\dagger} + \frac{\sigma}{\sqrt{N_C}}\mu_{\alpha/2}) \tag{14}$$

Under the $1-\alpha$ confidence level, the critical queuing time forecasting value is modified by (15).

$$t_\dagger^h = \begin{cases} \overline{\theta} & a_{f_{lf}} \geq 0 \text{ and } t_\dagger^h > \overline{\theta} \\ t_\dagger^h & \underline{\theta} \leq t_\dagger^h \leq \overline{\theta} \\ \underline{\theta} & a_{f_{lf}} < 0 \text{ and } t_\dagger^h < \underline{\theta} \end{cases} \tag{15}$$

where $a_{f_{lf}}$ is the one term coefficient of the fitting function (13).

The intuitionistic description of (15) is that, within the range of the rational critical queuing time values under certain confidence level, when the queue length trend has been increasing in the latest historical cycles, the critical queuing time of the current cycle should be no later than the maximum reliable value. On the contrary, when the queue length decreases in the past cycles, the critical queuing time of the current cycle should be no earlier than the minimum reliable value. By this restriction, the influence caused by traffic randomness can be weakened to higher level.

Suppose the forecasted critical queuing time of current cycle in (10) is denoted as $t_\dagger^c$, and the value based on historical cycles in (15) is denoted as $t_\dagger^h$, the final critical queuing time is calculated as follows:

$$t_\dagger = \mu t_\dagger^c + (1-\mu) t_\dagger^h \tag{16}$$

where μ is the weight coefficient.

As the analysis above, as long as the IPP samples are more than two CVs, the fitting forecasting method is available. When there are only two samples, the minimum weight coefficient for $t_\dagger^c$ is set as $\mu_{\min}$. With the growth of the number of samples, the real-time fitting forecasted value has been leading to a highly valuable weight compared with the historical data. As a conclusion, μ is assigned as follows:

$$\mu = \begin{cases} 0 & n < 2 \\ \mu_{\min} & n = 2 \\ \mu_{\min} + (1-\mu_{\min})[1 + e^{\lambda(-n+n_c)}]^{-1} & n > 2 \end{cases} \tag{17}$$

where $\mu_{\min}$ is the minimum weight value. n is the number of collected real-time IPP samples and n_c is the critical number. λ is the adjustment coefficient. Under different λ conditions, the weight value variation is presented as Fig. 6.

C. REAL-TIME QUEUE LENGTH ESTIMATION BASED ON MARKOV MODEL

As described in Section 2, as the queue length increases, the established time series consequentially shows non-stationary characteristics. In order to estimate the real-time queue

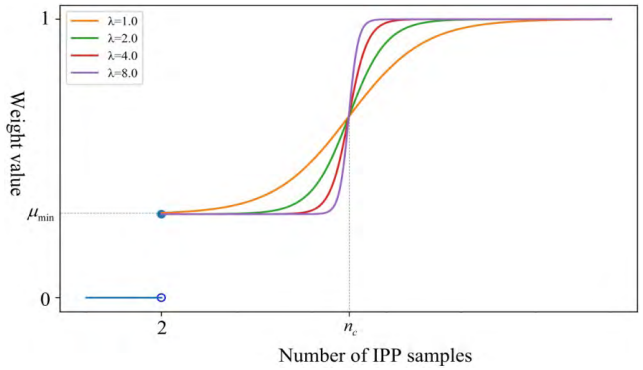

FIGURE 6. Weight coefficient value variation.

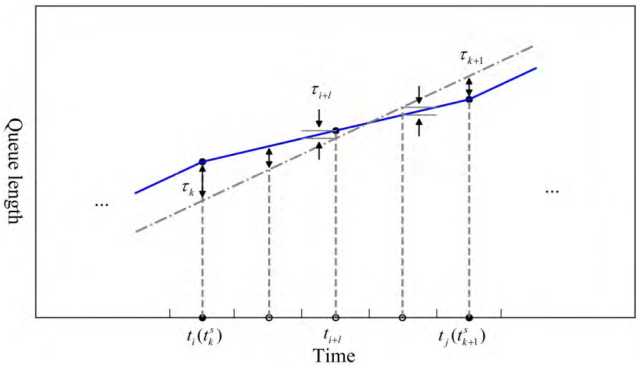

FIGURE 7. Compensation of queuing time series.

length, this paper initially takes a data transformation operation based on the historical vehicle average arrival rate to make the series trend to be stationary, and further builds a Markov chain for discretization analysis.

The real-time queuing time series is defined as (18).

$$T = \{\tau_1, \cdots, \tau_m, \cdots, \tau_M\} \tag{18}$$

where τ_m denotes the difference between the actual queuing number of vehicles and the theoretical vehicle arrival number at t_m, as shown in (19).

$$\tau_m = q(t_m) - u(t_m) \tag{19}$$

In (19), $u(t)$ is the statistical average vehicle arrival rate in the last N_C historical cycles.

The system makes a statistical analysis of the difference value of the latest N_C historical signal cycles and takes $[-\max|\tau_m|, \max|\tau_m|]$ as the error margin. Furthermore, the error margin is divided into N_e sequential sub-margins by unit 1, which represents one vehicle error, as is shown in (20).

$$\Omega = \{[-L, -L+1), \cdots, [-1, 0), [0, 1) \cdots, [L-1, L]\}_{1\times N_e} \tag{20}$$

where,

$$L = \lceil \max|\tau_m| \rceil, N_e = 2\lceil \max|\tau_m| \rceil \tag{21}$$

In Ω, suppose that each sub-margin corresponds with one error state, denoted as $\{e_1, e_2, \cdots, e_{N_e}\}$ respectively.

Similarly, the signal control cycle is divided into M sub-time periods by ΔT, $M = \lceil C/\Delta T \rceil$, where ΔT is the mean stopping interval and it is calculated by the stopping time of latest CV and the number of cumulative vehicles at that moment.

Since the sub-time period is divided by mean stopping interval, we can make an assumption that there is one vehicle stopping at the queue tail in each sub-time period. If the vehicle is a CV, then the difference value τ_k is calculated using (19) and correspond further with the certain state e_k. If there is no CV detected in the halfway period, supposing that there is virtual one is stopping at the half-way time and time series is compensated by keeping its integrity as shown in Fig. 7.

As aforementioned, there are total N_e states of the values of difference between the actual In each sub-time period of $[0, c]$, when a vehicle arrives at the queue tail, there are N_e transitions for the difference value states, that is, $e_i \to e_1$, $e_i \to e_2$, …, $e_i \to e_m$. Based on the previous N CVs, the Markov chain is built as follows:

Considering that the probability of the transition for the state e_i to e_j is:

$$p_{ij} = p(e_j|e_i) = p(e_i \to e_j) \tag{22}$$

The transition matrix for stopping states can be expressed by (23):

$$P^{(1)} = \begin{bmatrix} p_{11} & p_{12} & \cdots & p_{1N_e} \\ p_{21} & p_{22} & \cdots & p_{2N_e} \\ \vdots & \vdots & \ddots & \vdots \\ p_{N_e1} & p_{N_e2} & \cdots & p_{N_eN_e} \end{bmatrix} \tag{23}$$

The transition matrix calculated by the CVs in the current cycle is denoted as P', which is used for further queue length forecasting. In order to further decrease the influence caused by the random traffic characteristics to the queue length estimation error, an improved transition matrix considering the P' and the historical matrixes is used for the future k-steps forecasting. The improved transition matrix is presented in (24).

$$P = \eta P' + (1-\eta)(\gamma_1 P^1 + \cdots + \gamma_i P^i + \cdots + \gamma_{N_C} P^{N_C}) \tag{24}$$

where P^i is the transition matrix of the i^{th} former cycles ahead of the current. η is the weight coefficient for the current cycle, $0 < \eta < 1$, and presented in (25).

$$\eta = 1 - e^{-\zeta x^{\psi}} \tag{25}$$

In (25), ζ and ψ are the adjustment factors, x is the number of elements in queue length series at calculation point in the current cycle. When there are few elements at the forecasting point, the transition matrix established by these limited elements presents a smaller weight for forecasting operations,

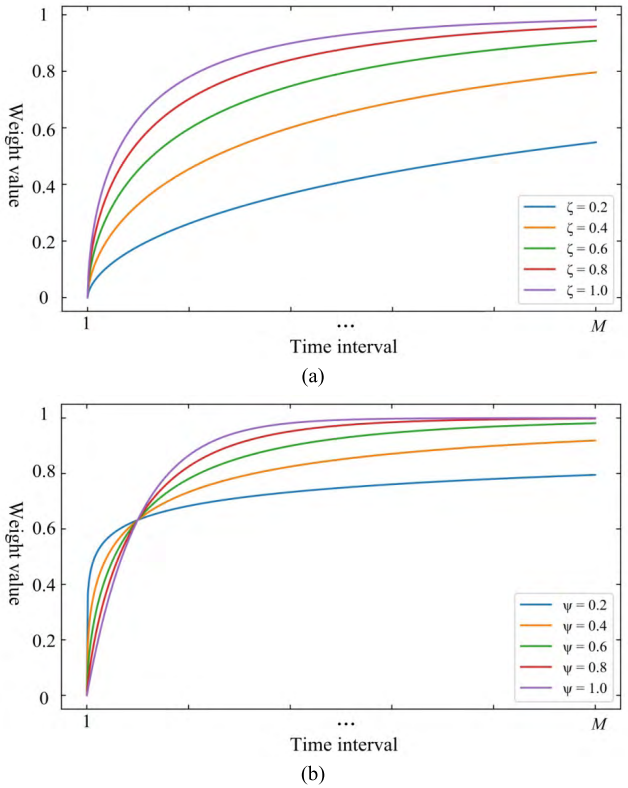

FIGURE 8. Weight distribution of the current signal cycle. (a) Weight variation under different ζ values ($\psi = 0.6$). (b) Weight variation under different ψ values ($\varsigma = 1$).

while the historical matrix gives a decisive effect. With the increase of number of elements, the matrix in the current cycles is more and more reliable for describing the real-time state transition characteristics. In this case, the impact of the current cycle increases while the historical data has a more moderate effect. The variation of the η is shown in Fig. 8.

In (24), γ_i is the normalized weight coefficient for historical cycles, $\sum_{i=1}^{N_C} \gamma_i = 1$. The cycle which is nearer to the current is assigned a higher weight. In this paper, we use the Gaussian function to assign values to weight coefficient.

$$\gamma_i = \frac{\gamma_i'}{\sum_{i=0}^{N_C} \gamma_i'} \tag{26}$$

where,

$$\gamma_i' = e^{-\rho(i-1)^\chi} \tag{27}$$

In (27), ρ is the accommodation coefficient. Suppose that the minimum weight confidence level is ε when $i = N_C$, the accommodation coefficient is calculated as follows:

$$\gamma_{N_C}' = e^{-\rho(N_C-1)^\chi} \le \varepsilon \tag{28}$$

$$\rho \ge -\frac{\ln \varepsilon}{(N_C-1)^\chi} \tag{29}$$

The weight distribution is shown in Fig. 9.

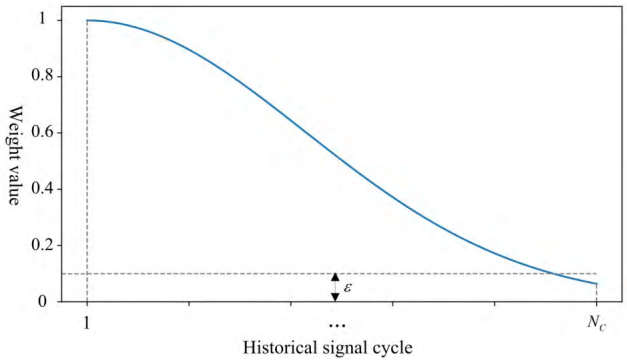

FIGURE 9. Weight distribution of different historical signal cycles.

In summary, the improved transition matrix is expressed by (30), as shown at the bottom of the next page, and the k-step transition matrix is expressed by (31), as shown at the bottom of the next page.

Suppose that the difference value state at t_N^s is e_i, the initial state probability vector can be expressed by (32).

$$\Pi(0) = (\pi_1(0), \pi_2(0), \cdots, \pi_{N_e}(0)) \tag{32}$$

where $\pi_i(0) = 1$, $\pi_{1\sim i-1, i+1\sim N_e}(0) = 0$.

At the critical queuing time $t_\dagger$, the transition steps $k = \lceil (t_\dagger - t_N^s)/\Delta t \rceil$, and the state probability vector at $t_\dagger$ is expressed by (33).

$$\Pi(k) = \Pi(0)P^{(k)} = (\pi_1(k), \pi_2(k), \cdots, \pi_{N_e}(k)) \tag{33}$$

Suppose that the state of $\max_{i=1}^{N_e}\{\pi_i(k)\}$ is $e_\dagger$ and the corresponding difference value is $\tau_\dagger$, based on (19), the forecasting queue length is calculated by (34).

$$q(t_\dagger) = u(t_\dagger) + \tau_\dagger \tag{34}$$

where $u(t_\dagger)$ denotes the number of queuing vehicles at the critical queuing time $t_\dagger$ referring to the statistical average vehicle arrival rate.

IV. CASE STUDY

To evaluate the proposed method, a case study is presented with an example intersection at the Hongkong Road-Fuzhou Road of Qingdao City of China (Fig. 10). The trajectory of vehicles and the queuing process are obtained from the high-definition video camera.

The background details of the intersection are introduced as follows:

A. ROAD CHANNELIZATION

The case entrance lane contains three through lanes and two left-turn lanes. The middle two through lanes are selected for the case study.

B. BACKGROUND TRAFFIC SIGNAL PLAN

The signal control cycle is 154s and the phase-time of through direction is 43s, as is shown in Fig. 11.

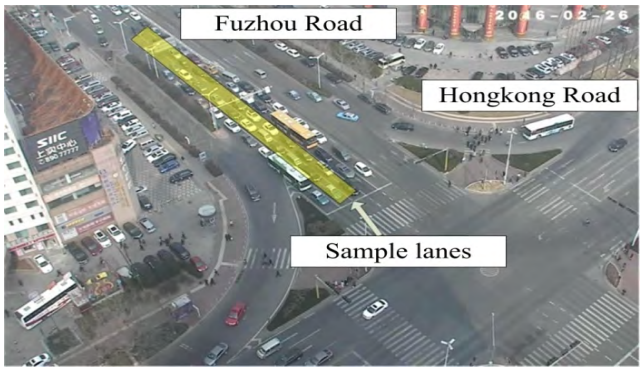

FIGURE 10. The sample Case example of an intersection.

C. TRAFFIC FLOW VOLUME CHARACTERISTICS

The analysis time period is chosen at 12:00-14:00 in which the traffic is unsaturated. The statistical analysis to get the traffic volume by high-definition video where the hourly volume is 441 veh/h. The variation of traffic volume per cycle is shown in Fig. 12.

As an example, the five cycles mentioned in Fig. 12 are selected for studying the case further.

D. STABILITY ANALYSIS OF QUEUE LENGTH SERIES

From Fig. 12, we can see that, the traffic volume values in the chosen five cycles change dynamically, presenting a typical random feature. Under 60% penetration rate of CVs, the samples are selected using a random method. And for the fifth cycle in case cycles, the CVs are also randomly selected at the penetration rate of 20%, 40%, 60% and 80% respectively. For instance, part of the CVs distributions in different cycles are presented in Fig. 13.

Using the method proposed, the time series is built and the stability characteristics are analyzed by ADF test. The results are shown in TABLE 1 and TABLE 2.

From the ADF test results, it is found that, the original difference value series of the case intersection, where the value is calculated by the difference between the actual queuing number of vehicles and the theoretical vehicle arrival number, are all still non-stationary. This phenomenon is mainly caused by the short-term vehicle arrival behavior which is influenced by some time-invariant and time-varying features.

Under 60% penetration rate, the first-order differences of the original difference value series in the five case cycles all present stationary at 5% level. Besides, in the fifth cycle, the first-order or second-order differences under different penetration rates are also present stationary. This verifies that the proposed queue length series construction method is able to model the random characteristic of the traffic flow and the translation to be stationary provides a feasible method for real-time queue length estimation.

To illustrate this aspect further, in TABLE 2, when the penetration rates are 20% and 40%, a second-order difference calculation must be performed to make the original series stationary. While at 20%, the time series itself is just stationary for Lane 2. Compared with other situations, these extreme differences mainly caused by the less number of samples at low penetration rate conditions, where these samples are not enough to describe the queuing process. The random distributions of the samples may cause different series with entirely variation trends. For any cases, these series can be made stationary by different operations.

E. ANALYSIS OF THE QUEUE LENGTH ESTIMATION RESULTS

The fifth cycle is taken as an example to verify the performance of the proposed method under penetration rate of 60%. As is described in Section 3, two kinds of transition matrixes are used for the Markov forecasting model in this paper, the transition matrix (TM for short, as (23)) based

$$P^{(1)} = \begin{bmatrix} \gamma_0 p'_{11} + \sum_{i=1}^{N_C} \gamma_i p^i_{11} & \gamma_0 p_{12} + \sum_{i=1}^{N_C} \gamma_i p^i_{12} & \cdots & \gamma_0 p_{1N_e} + \sum_{i=1}^{N_C} \gamma_i p^i_{1N_e} \\ \gamma_0 p'_{21} + \sum_{i=1}^{N_C} \gamma_i p^i_{21} & \gamma_0 p_{22} + \sum_{i=1}^{N_C} \gamma_i p^i_{21} & \cdots & \gamma_0 p_{2N_e} + \sum_{i=1}^{N_C} \gamma_i p^i_{2N_e} \\ \vdots & \vdots & \ddots & \vdots \\ \gamma_0 p'_{N_e1} + \sum_{i=1}^{N_C} \gamma_i p^i_{N_e1} & \gamma_0 p_{N_e2} + \sum_{i=1}^{N_C} \gamma_i p^i_{N_e2} & \cdots & \gamma_0 p_{N_eN_e} + \sum_{i=1}^{N_C} \gamma_i p^i_{N_eN_e} \end{bmatrix} \tag{30}$$

$$P^{(k)} = P^k = \begin{bmatrix} \gamma_0 p'_{11} + \sum_{i=1}^{N_C} \gamma_i p^i_{11} & \gamma_0 p_{12} + \sum_{i=1}^{N_C} \gamma_i p^i_{12} & \cdots & \gamma_0 p_{1N_e} + \sum_{i=1}^{N_C} \gamma_i p^i_{1N_e} \\ \gamma_0 p'_{21} + \sum_{i=1}^{N_C} \gamma_i p^i_{21} & \gamma_0 p_{22} + \sum_{i=1}^{N_C} \gamma_i p^i_{21} & \cdots & \gamma_0 p_{2N_e} + \sum_{i=1}^{N_C} \gamma_i p^i_{2N_e} \\ \vdots & \vdots & \ddots & \vdots \\ \gamma_0 p'_{N_e1} + \sum_{i=1}^{N_C} \gamma_i p^i_{N_e1} & \gamma_0 p_{N_e2} + \sum_{i=1}^{N_C} \gamma_i p^i_{N_e2} & \cdots & \gamma_0 p_{N_eN_e} + \sum_{i=1}^{N_C} \gamma_i p^i_{N_eN_e} \end{bmatrix}^k \tag{31}$$

TABLE 1. Adf test results of different cycles (60% penetration rate).

Cycle	Series type	Root test content		Values for different lanes	
				Lane 1	Lane 2
The first cycle	Original difference value series (T)	ADF test values		-1.0935	-2.2840
		Tested critical values	1% level	-2.7922	-2.8473
			5% level	-1.9777	-1.9882
	First-order difference of T	ADF test values		-2.9166	-3.2089
		Tested critical values	1% level	-2.8167	-4.2971
			5% level	-1.9823	-3.2127
The second cycle	Original difference value series (T)	ADF test values		-2.6904	-3.2963
		Tested critical values	1% level	-5.5219	-4.1220
			5% level	-4.1078	-3.1449
	First-order difference of T	ADF test values		-2.3938	-2.0696
		Tested critical values	1% level	-2.8167	-2.7922
			5% level	-1.9823	-1.9777
The third cycle	Original difference value series (T)	ADF test values		-0.5679	-1.3671
		Tested critical values	1% level	-2.7922	-2.8167
			5% level	-1.9777	-1.9823
	First-order difference of T	ADF test values		-2.0516	-3.0718
		Tested critical values	1% level	-2.8473	-2.8473
			5% level	-1.9882	-1.9882
The fourth cycle	Original difference value series (T)	ADF test values		-0.8216	-0.9824
		Tested critical values	1% level	-2.7719	-2.7719
			5% level	-1.9740	-1.9740
	First-order difference of T	ADF test values		-4.2489	-2.1002
		Tested critical values	1% level	-2.8473	-2.7922
			5% level	-1.9882	-1.9777
The fifth cycle	Original difference value series (T)	ADF test values		0.9808	0.3645
		Tested critical values	1% level	-2.7719	-2.8473
			5% level	-1.9740	-1.9882
	First-order difference of T	ADF test values		-5.0444	-5.3340
		Tested critical values	1% level	-5.5219	-6.2921
			5% level	-4.1078	-4.4504

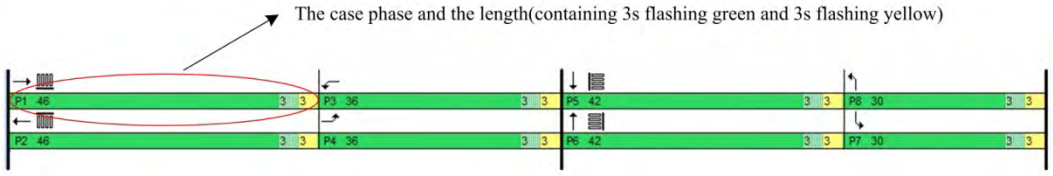

FIGURE 11. Signal time plan of the case intersection.

on the queue length time series of CVs in the current signal cycle, and the comprehensive transition matrix (CTM for short, as (30)) based on the TMs of the current cycle and the historical cycles. Using the Markov model, the difference values between the theoretical and actual queue length are estimated based on two kinds of transition matrixes and the results are shown in Fig. 14. As shown, the referenced original series is obtained when penetration rate is 100%, that is, all the vehicles on road are connected vehicles.

From the results shown in Fig. 14, it is evident that, both of the two estimation curves appropriately match the actual value. However, in the early stage of the signal cycle, the errors are generally larger than the later stage due to

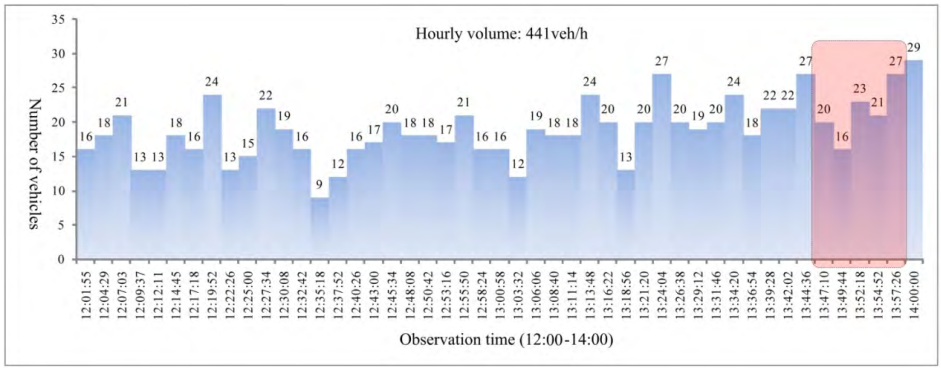

FIGURE 12. Variation of traffic volume.

TABLE 2. Adf test results of the fifth cycle.

Penetration rate	Series type	Root test content		Values for different lanes	
				Lane 1	Lane 2
20%	Original different value series (T)	ADF test values		0.0401	-2.0792
		Tested critical values	1% level	-2.8167	-2.8861
			5% level	-1.9823	-1.9959
	First-order difference of T	ADF test values		-2.7415	-NA-
		Tested critical values	1% level	-5.8352	-NA-
			5% level	-4.2465	-NA-
	Second-order difference of T	ADF test values		-2.3967	-NA-
		Tested critical values	1% level	-2.8473	-NA-
			5% level	-1.9882	-NA-
40%	Original different value series (T)	ADF test values		-0.1048	3.1091
		Tested critical values	1% level	-2.7719	-2.7719
			5% level	-1.9740	-1.9740
	First-order difference of T	ADF test values		-3.3360	-2.9931
		Tested critical values	1% level	-2.7922	-5.1249
			5% level	-1.9777	-3.4200
	Second-order difference of T	ADF test values		-NA-	-6.0606
		Tested critical values	1% level	-NA-	-4.2971
			5% level	-NA-	-3.2127
60%	Original different value series (T)	ADF test values		0.9808	0.3645
		Tested critical values	1% level	-2.7719	-2.8473
			5% level	-1.9740	-1.9882
	First-order difference of T	ADF test values		-5.0444	-5.3340
		Tested critical values	1% level	-5.5219	-6.2921
			5% level	-4.1078	-4.4504
80%	Original different value series (T)	ADF test values		-3.6191	-0.2610
		Tested critical values	1% level	-5.1249	-2.8167
			5% level	-3.8333	-1.9823
	First-order difference of T	ADF test values		-2.1149	-6.3682
		Tested critical values	1% level	-2.7922	-5.1249
			5% level	-1.9778	-3.9334

only a few number of samples. With the time increases, more CVs are detected and the queue time series present a much stronger relevant characteristic. To provide a quantitative evaluation, the root mean squared errors (RMSE) of the two estimation methods are calculated and shown in TABLE 3.

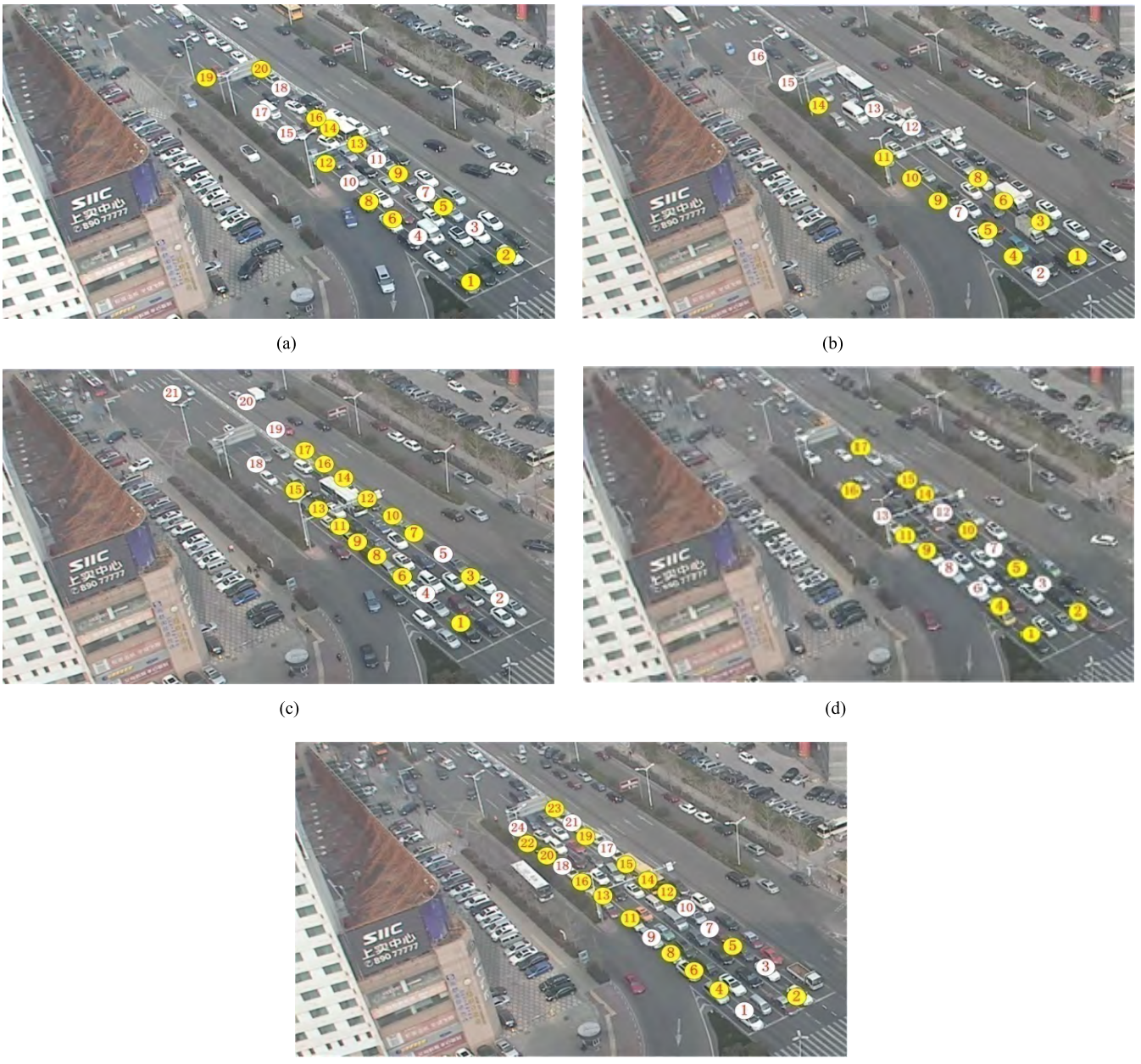

FIGURE 13. CVs distribution examples under different penetration rates (yellow number represents CV). (a) The first cycle. (b) The second cycle. (c) The third cycle. (d) The fourth cycle. (e) The fifth cycle.

TABLE 3. RMSEs of the two estimation methods for difference error (number of vehicles).

Estimation method	Lane 1	Lane 2	Average value
Markov model based on TM	0.198	0.193	0.1955
Markov model based on CTM	0.198	0.169	0.1835
Improvement	0%	12.4%	6.2%

From TABLE 3, we can see that, the estimation errors can reach a decimal level (less than 0.2 vehicles in the case study). Furthermore, the Markov model based on CTM provides a more accurate estimation result compared with the model based on TM. The CTM makes great impact to alleviate the effect caused by the random distributions of CVs when there

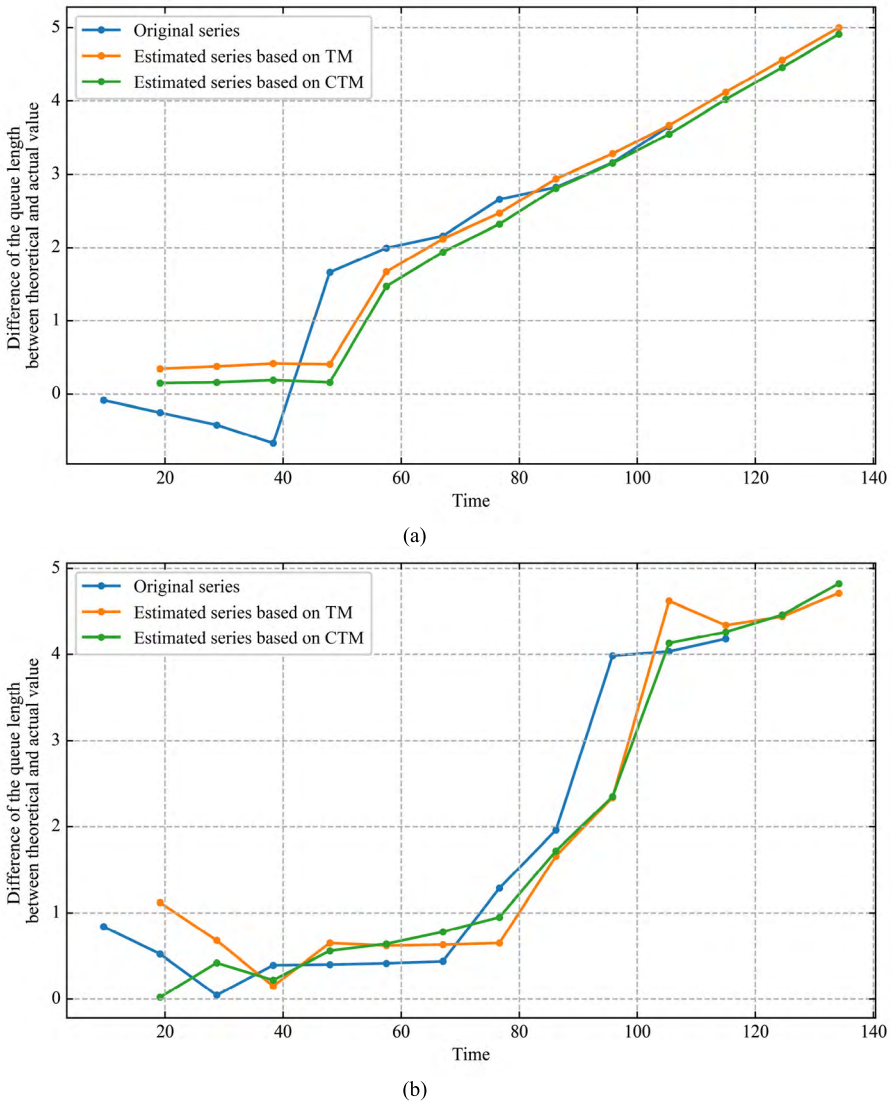

FIGURE 14. Difference value estimation results. (a) Lane 1. (b) Lane 2.

TABLE 4. RMSEs of the two estimation methods for queue length (number of vehicles).

Estimation method	Lane 1	Lane 2	Average value
Markov model based on TM	0.213	0.207	0.21
Markov model based on CTM	0.209	0.169	0.189
Improvement	1.9%	18.4%	10.1%

are only a few samples, especially in the early stage of the signal cycle.

Further, based on the difference estimation results, the real-time queue length estimation results and the critical queue length forecasting results are presented in Fig. 15.

From the results shown in Fig. 15, it is evident that, the queuing estimation curves appropriately fit the actual queue length using the CV stopping states. To give a quantitative evaluation, the RMSEs of the two estimation methods are calculated and shown in TABLE 4.

From TABLE 4, we can see that, the Markov model based on the CTM provides a more accurate estimation result compared with the model based on TM. This result shows consistent with the conclusions in TABLE 3. Moreover, we use gray correlation analysis method to further study the queue variations to the actual scenario of the two proposed methods.

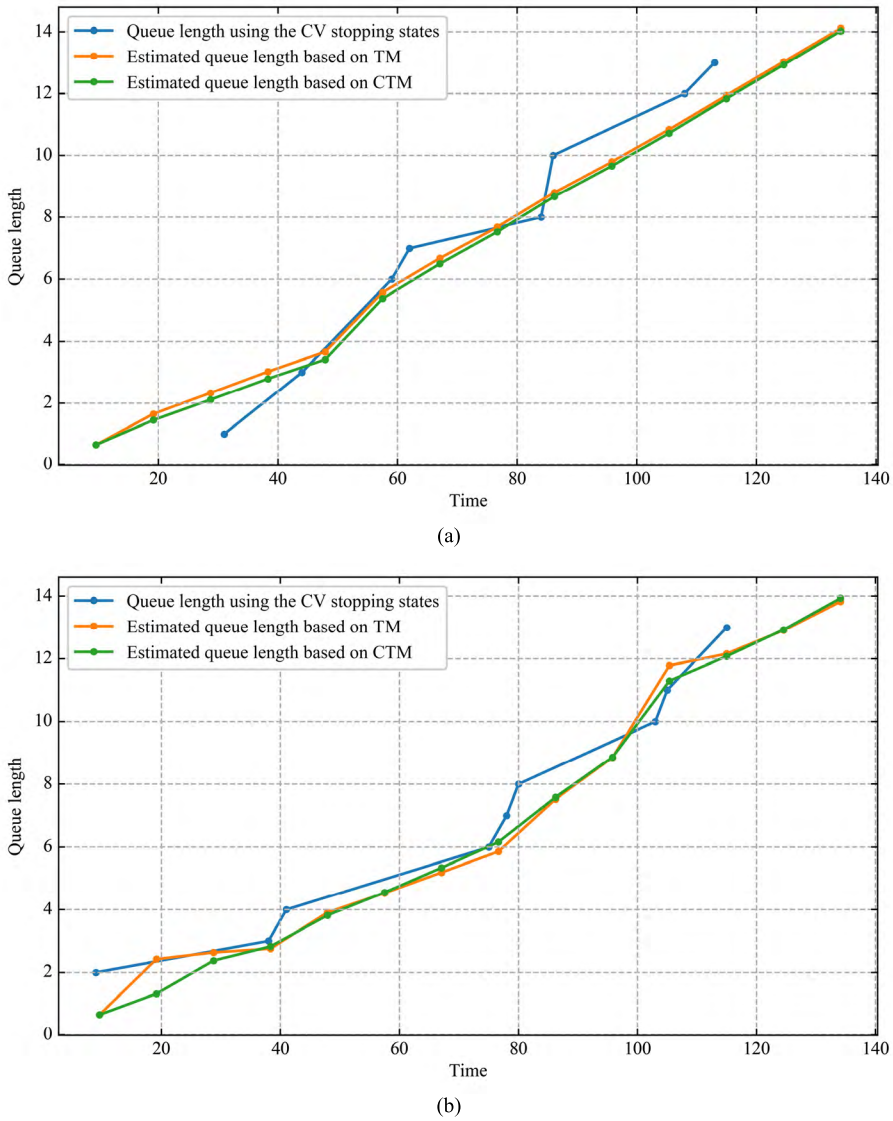

FIGURE 15. Real-time queue length estimation and the critical queue length forecasting results. (a) Lane 1. (b) Lane 2.

Suppose the series of the characteristic behaviors (the queue length series using the CV stopping states in the case study) are:

$$X_0(k) = (x_0(1), x_0(2), \cdots, x_0(n)) \tag{35}$$

The series of relevant factors (two estimated queue length series based on Markov model) are:

$$X_i(k) = (x_i(1), x_i(2), \cdots, x_i(n)) \tag{36}$$

The displacement difference of series X_0 and X_i at the point k can be expressed by (37).

$$\Delta x_{0i}(k) = x_0(k) - x_i(k) \tag{37}$$

$|\Delta x_{0i}(k)|$ is the absolute difference which represents the close degree for the two series at the point k. The smaller the value of $|\Delta x_{0i}(k)|$ is, the closer the two lines are.

The correlation degree for X_i and X_0 is expressed by (38).

$$\gamma(X_0, X_i) = \sum_{k=1}^{n} \omega_k \gamma(x_0(k), x_i(k)) \tag{38}$$

In (38), ω_k is the weight. $\gamma(x_0(k), x_i(k))$ is the correlation coefficient, which is calculated by (39).

$$\gamma(x_0(k), x_i(k)) = \frac{\min\limits_i \min\limits_k |\Delta x_{0i}(k)| + \rho \max\limits_i \max\limits_k |\Delta x_{0i}(k)|}{|\Delta x_{0i}(k)| + \rho \max\limits_i \max\limits_k |\Delta x_{0i}(k)|} \tag{39}$$

where $\min\limits_i \min\limits_k |\Delta x_{0i}(k)|$ is the minimum difference and $\max\limits_i \max\limits_k |\Delta x_{0i}(k)|$ is the maximum difference. ρ is the resolution ration, and $\rho \in [0, 1]$. The valuing method of ρ refers to [27].

From (39), the average gray relational degree of the estimation results based on the current cycle is 0.682 for Lane 1, and the value for Lane 2 is 0.693. The results show a highly consistency compared to earlies research.

V. CONCLUSIONS AND FUTURE WORK

In the CV environment, the trajectory information of the CVs provides a new data resource to estimate the real-time queue length at signalized intersection. In this paper, the anchor message when the CV stops is fully used and a real-time queue length estimation using the time series analysis is proposed. The method includes two steps: queue length series construction and real-time queue length estimation. The queue length time series can appropriately describe the random variations of traffic flow. Besides, the optimized state transition matrix considering the current cycle and the historical cycles makes up for the randomness when the number of CV samples is small and improves the accuracy for queue length estimation.

The proposed method is tested in actual traffic scenario. Under different cycles and penetration rates, the stationary characteristic is analyzed and the results verify that the queue length series is possible to be forecasted after certain order difference process. Further estimation results using the Markov model shows that, the proposed method provides a reasonable and more accurate real-time queue length forecasting value.

We believe that this approach can be practically applied to a number of real-time applications such as traffic congestion evaluation, traffic guidance, and signal control which rely on the accuracy of queue length. To further mining the detailed random characteristics of traffic flow to influence the performance the proposed method, our future work is mainly focused on the impact of queue length estimation accuracy caused by different CV distributions in the queue, for instance, the concentrated distribution, the uniform distribution or other distributions etc.

REFERENCES

[1] H. A. E. Ai-Jameel and M. A. H. Ai-Jumaili, "Analysis of traffic stream characteristics using loop detector data," *Jordan J. Civil Eng.*, vol. 10, no. 4, pp. 403–416, 2016.

[2] K. Yang, R. J. Yu, and X. S. Wang, "Application of aggregated lane traffic data from dual-loop detector to crash risk evaluation," (in Chinese), *J. Tongji Univ.*, vol. 44, no. 10, pp. 1567–1572, 2016.

[3] J. J. Lamas-Seco *et al.*, "Multi-loop inductive sensor model for vehicle traffic applications," *Sens. Actuators A, Phys.*, vol. 263, pp. 580–592, Aug. 2017.

[4] T.-J. Ho and M.-J. Chung, "An approach to traffic flow detection improvements of non-contact microwave radar detectors," in *Proc. Int. Conf. Appl. Syst. Innov.*, May 2016, pp. 1–4.

[5] Z. W. Li, J. Zhang, and H. Gu, "Real-time traffic speed estimation with adaptive cruise control vehicles and manual vehicles in a mixed environment," in *Proc. 16th COTA Int. Conf. Transp. Professionals*, 2016, pp. 51–62.

[6] Q. Wang, J. Zheng, H. Xu, B. Xu, and R. Chen, "Roadside magnetic sensor system for vehicle detection in urban environments," *IEEE Trans. Intell. Transp. Syst.*, vol. 19, no. 5, pp. 1365–1374, May 2017.

[7] J. A. Sanguesa *et al.*, "Sensing traffic density combining V2V and V2I wireless communications," *Sensors*, vol. 15, no. 12, pp. 31794–31810, 2015.

[8] J. Barrachina, P. Garrido, M. Fogue, F. J. Martinez, J.-J. Cano, and C. T. Calafate, "A V2I-based real-time traffic density estimation system in urban scenarios," *Wireless Pers. Commun.*, vol. 8, no. 1, pp. 259–280, 2015.

[9] R. A. Mallah, A. Quintero, and B. Farooq, "Distributed classification of urban congestion using VANET," *IEEE Trans. Intell. Transp. Syst.*, vol. 18, no. 9, pp. 2435–2442, Sep. 2017.

[10] S. R. Hussain, A. Odeh, A. Shivakumar, S. Chauhan, and K. Harfoush, "Real-time traffic congestion management and deadlock avoidance for vehicular ad Hoc networks," in *Proc. High Capacity Opt. Netw. Emerg./Enabling Technol.*, 2013, pp. 223–227.

[11] W. C. Chan, T.-C. Lu, and R.-J. Chen, "Pollaczek-Khinchin formula for the M/G/1 queue in discrete time with vacations," *IEE Proc.-Comput. Digit. Techn.*, vol. 144, no. 4, pp. 222–226, 1997.

[12] D. J. Fagnant and K. M. Kockelman, "Dynamic ride-sharing and fleet sizing for a system of shared autonomous vehicles in Austin, Texas," *Transportation*, vol. 45, no. 1, pp. 143–158, 2018.

[13] H. Al-Khateeb *et al.*, "Proactive threat detection for connected cars using recursive Bayesian estimation," *IEEE Sensors J.*, vol. 18, no. 12, pp. 4822–4831, Jun. 2018.

[14] M. S. Iqbal, M. Hadi, and Y. Xiao, "Effect of link-level variations of connected vehicles (CV) proportions on the accuracy and reliability of travel time estimation," *IEEE Trans. Intell. Transp. Syst.*, vol. 20, no. 1, pp. 87–96, Jan. 2018.

[15] L. Chai, B. Cai, W. ShangGuan, and J. Wang, "Simulation and testing method for evaluating the effects of position error, communication delay and penetration rate to connected vehicles safety," in *Proc. Chin. Automat. Congr.*, Jinan, China, Oct. 2017, pp. 4389–4394.

[16] F. A. Silva, A. A. F. Loureiro, and L. B. Ruiz, "Content replication in mobile vehicular ad-hoc networks," in *Proc. 16th IEEE Int. Conf. Mobile Data Manage.*, Pittsburgh, PA, USA, Jun. 2015, pp. 26–29.

[17] G. Comert and M. Cetin, "Queue length estimation from probe vehicle location and the impacts of sample size," *Eur. J. Oper. Res.*, vol. 197, no. 1, pp. 196–202, 2009.

[18] G. Comert and M. Cetin, "Analytical evaluation of the error in queue length estimation at traffic signals from probe vehicle data," *IEEE Trans. Intell. Transp. Syst.*, vol. 12, no. 2, pp. 563–573, Jun. 2011.

[19] F. Li, K. Tang, and J. R. Yao, "Real-time queue length estimation for signalized intersections using vehicle trajectory data," *Transp. Rec. J., Transp. Res. Board*, vol. 2623, pp. 49–59, 2017.

[20] K. Tiaprasert, Y. Zhang, X. B. Wang, and X. Zeng, "Queue length estimation using connected vehicle technology for adaptive signal control," *IEEE Trans. Intell. Transp. Syst.*, vol. 16, no. 4, pp. 2129–2140, Aug. 2015.

[21] X. Lin *et al.*, "Improved road-network-flow control strategy based on macroscopic fundamental diagrams and queuing length in connected-vehicle network," *Math. Problems Eng.*, vol. 2017, no. 1, 2017, Art. no. 8784067.

[22] R. Doolan and G. M. Muntean, "EcoTrec—A novel VANET-based approach to reducing vehicle emissions," *IEEE Trans. Intell. Transp. Syst.*, vol. 18, no. 3, pp. 608–620, Mar. 2017.

[23] M. Wang, W. Daamen, S. P. Hoogendoorn, and B. van Arem, "Connected variable speed limits control and car-following control with vehicle-infrastructure communication to resolve stop-and-go waves," *J. Intell. Transp. Syst.*, vol. 20, no. 6, pp. 559–572, 2016.

[24] J. Ding, H. Xu, J. Hu, and Y. Zhang, "The impact of centralized cooperative intersection control on traffic flow characteristics," in *Proc. 4th Int. Conf. Transp. Inf. Safety*, Aug. 2017, pp. 858–864.

[25] M. R. Shahrbabaki, A. A. Safavi, M. Papageorgiou, and I. Papamichail, "A data fusion approach for real-time traffic state estimation in urban signalized links," *Transp. Res. C, Emerg. Technol.*, vol. 92, pp. 525–548, Jul. 2018.

[26] H. Liu, L. Rai, J. Wang, and C. Ren, "A new approach for real-time traffic delay estimation based on cooperative vehicle-infrastructure systems at the signal intersection," *Arabian J. Sci. Eng.*, Jun. 2018.

[27] H. Liu, N. Li, D. Guan, and L. Rai, "Data feature analysis of non-scanning multi target millimeter-wave radar in traffic flow detection applications," *Sensors*, vol. 18, no. 9, p. 2756, 2018.

HAIQING LIU (M'18) received the bachelor's degree in automation from Central South University, China, in 2008, and the Ph.D. degree in system engineering from Shandong University, China, in 2015. From 2015 to 2017, he was a postdoctoral researcher with the Postdoctoral Work Station, Hisense Group, China. He is currently a Lecturer with the Shandong University of Science and Technology. His current research interests include traffic engineering and control, cooperative vehicle infrastructure systems, and traffic intelligent perception.

WENLI LIANG was born in Qingdao, China, in 1996. She received the bachelor's degree in traffic engineering from Shandong Jiaotong University, China, in 2018. She is currently pursuing the master's degree with the Shandong University of Science and Technology, China. Her current research interest includes logistics engineering.

LAXMISHA RAI (S'05–M'08–SM'16) received the B.E. degree in computer engineering from Mangalore University, Mangalore, India, in 1998, the M.Tech. degree in computer science and engineering from the Manipal Institute of Technology, Manipal, India, in 2001, and the Ph.D. degree in electronics from Kyungpook National University, Daegu, South Korea, in 2008.

From 2008 to 2009, he was a Postdoctoral Researcher with Soongsil University, South Korea. He is currently a Professor with the College of Electronics, Communication, and Physics, Shandong University of Science and Technology, Qingdao, China. He has published over 50 peer-reviewed research papers in international journals and conferences. He has published three books titled *Programming in Java With Object-Oriented Features*, *MOOCs: Effective Teaching and Learning Strategies* (both published by the China University of Petroleum), and *Programming in C++: Object-Oriented Features* (China Science Publishing, Beijing, and De Gruyter Publishers, Germany). He is an Author of two patents (U.S. and South Korean). His research interests include software engineering, real-time systems, embedded systems, autonomous mobile robots, expert systems, wireless sensor networks, MOOC, and bilingual education. He is currently serving as an Associate Editor for the IEEE ACCESS JOURNAL.

KUNMIN TENG (S'18) received the bachelor's degree from the Shandong University of Science and Technology, in 2018, where he is currently pursuing the master's degree. His current research interest includes the traffic information control and engineering.

SHENGLI WANG received the Ph.D. degree in instrument science and technology from Southeast University, China, in 2013. From 2015 to 2017, he was the Chief Engineer with Shandong Astro-Compass Information Technology Co., Ltd. He is currently an Associate Professor with the Shandong University of Science and Technology. His current research interests include traffic engineering and control, cooperative vehicle infrastructure systems, and co-location.